Published in final edited form as:
Invest Ophthalmol Vis Sci. 2009 September ; 50(9): 4033–4044. doi:10.1167/iovs.08-3162.

Effects of Form Deprivation on Peripheral Refractions and Ocular Shape in Infant Rhesus Monkeys (*Macaca mulatta*)

Juan Huang[1,2], **Li-Fang Hung**[1,2], **Ramkumar Ramamirtham**[1,2,3], **Terry L. Blasdel**[4], **Tammy L. Humbird**[4], **Kurt H. Bockhorst**[5], and **Earl L. Smith III**[1,2]

[1]College of Optometry, University of Houston, Houston, Texas

[2]Vision CRC, Sydney, Australia.

[4]Animal Care Operations, University of Houston, Houston, Texas

[5]Department of Diagnostic & Interventional Imaging, University of Texas at Houston Medical School, Houston, Texas

Abstract

Purpose—To determine whether visual experience can alter ocular shape and peripheral refractive error pattern, the authors investigated the effects of form deprivation on refractive development in infant rhesus monkeys.

Methods—Monocular form deprivation was imposed in 10 rhesus monkeys by securing diffuser lenses in front of their treated eyes between 22 ± 2 and 163 ± 17 days of age. Each eye's refractive status was measured longitudinally by retinoscopy along the pupillary axis and at 15° intervals along the horizontal meridian to eccentricities of 45°. Control data for peripheral refraction were obtained from the nontreated fellow eyes and six untreated monkeys. Near the end of the diffuser-rearing period, the shape of the posterior globe was assessed by magnetic resonance imaging. Central axial dimensions were also determined by A-scan ultrasonography.

Results—Form deprivation produced interocular differences in central refractive errors that varied between +2.69 and –10.31 D (treated eye–fellow eye). All seven diffuser-reared monkeys that developed at least 2.00 D of relative central axial myopia also showed relative hyperopia in the periphery that increased in magnitude with eccentricity. Alterations in peripheral refraction were highly correlated with eccentricity-dependent changes in vitreous chamber depth and the shape of the posterior globe.

Conclusions—Like humans with myopia, monkeys with form-deprivation myopia exhibit relative peripheral hyperopia and eyes that are less oblate and more prolate. Thus, in addition to producing central refractive errors, abnormal visual experience can alter the shape of the posterior globe and the pattern of peripheral refractive errors in infant primates.

Studies of refractive development, particularly those concerned with the role of vision in the genesis of common refractive errors, have historically focused on the refractive status at the fovea (for a review, see Ref. 1). However, in addition to the increase in radial astigmatism with eccentricity, spherical-equivalent refractive error can vary substantially across the visual field.

Corresponding author: Earl L. Smith III, College of Optometry, University of Houston, 505 J Armistead Building, Houston, TX 77204-2020; esmith@uh.edu..
[3]Present affiliation: Alcon Laboratories, Inc., Fort Worth, Texas.

Disclosure: **J. Huang**, None; **L.-F. Hung**, None; **R. Ramamirtham**, None; **T.L. Blasdel**, None; **T.L. Humbird**, None; **K.H. Bockhorst**, None; **E.L. Smith III**, P

1–12 The magnitude of these peripheral refractive errors is often sufficient to degrade peripheral visual performance.13,14

There is additional interest in peripheral refraction because peripheral refractive errors may contribute to the development of common axial refractive errors.15–20 In particular, the pattern of peripheral refractive errors may play a role in the onset and progression of myopia. For example, in comparison with children and adults with emmetropia and hyperopia, those with myopia at the fovea typically demonstrate less myopia or more hyperopia in the periphery,4, 5,21 and the magnitude of this relative peripheral hyperopia increases with the degree of axial myopia.22,23 It is possible that the association between peripheral hyperopia and central myopia is causal because relative peripheral hyperopia often precedes the onset or progression of central myopia in humans15,17,18 and because experimentally imposed peripheral hyperopic defocus can produce central axial myopia in infant monkeys (Smith EL III, et al. *IOVS* 2007;48:ARVO E-Abstract 1533).

Although peripheral refractions are dependent on anterior segment optics and geometry, variations in the pattern of peripheral refraction as a function of central refractive error are thought to primarily reflect differences in the shape of the posterior globe.23–25 Despite some inconsistencies between studies1 and possible meridional variations within eyes,23 it appears that subjects with myopia exhibit relative hyperopia in the periphery because the posterior poles of their eyes are relatively prolate, whereas the relative peripheral myopia in those with axial hyperopia occurs because their eyes are relatively oblate (Gilmartin B, et al. *IOVS* 2007;48:ARVO E-Abstract 1215).23

Littleis known about why subjects with myopia and those with hyperopia have differently shaped eyes or how these differences develop over time. It has been argued that some of these differences in posterior globe shape are associated with absolute differences in axial length and are probably a consequence of a preprogrammed genetic growth process.26 Shape differences may also arise during eye growth as a result of mechanical factors21,23,27,28 and/or regional variations in the mechanical properties of the sclera.29,30 It is also possible, however, that differences in posterior globe shape come about as a consequence of selective visual experience operating through local retinal mechanisms10,22,23 (Flitcroft DI. *IOVS* 2006;47:ARVO E-Abstract 4778) and/or of regional variations in the number, density, or effectiveness of vision-dependent regulatory mechanisms.31,32

Visual experience can have dramatic effects on central refractive errors, and it is reasonable to expect that changes in the eye's optical and axial dimensions responsible for changes in central refraction also affect peripheral refraction. In this respect, it has recently been reported that the more myopic eyes of marmosets with vision-induced anisometropia exhibit relative hyperopia in the temporal field, but not in the nasal field (Totonelly KC, et al. *IOVS* 2008;49:ARVO E-Abstract 3589). The aims of this investigation were to determine whether the pattern of peripheral refraction and the shape of the posterior globe are influenced by visual experience in young rhesus monkeys and whether the patterns of peripheral refractive errors in macaques with experimentally induced central refractive errors are similar to those observed in humans.

Materials and Methods

Subjects

The primary subjects of this study were 16 infant rhesus monkeys (*Macaca mulatta*) obtained at approximately 2 to 3 weeks of age and housed in our primate nursery, which was maintained at a 12-hour light/12-hour dark cycle.33 All rearing and experimental procedures were reviewed and approved by the University of Houston's Institutional Animal Care and Use

Committee and were in compliance with the ARVO Statement for the Use of Animals in Ophthalmic and Vision Research.

Monocular form deprivation was produced in 10 infant monkeys by securing a diffuser spectacle lens in front of one eye; a clear Plano lens was positioned in front of the fellow eye (see Refs. 34,35 for details). The diffuser lenses, which consisted of a zero-powered carrier lens covered with a commercially available occlusion foil (Bangerter Occlusion Foils; Fresnel Prism and Lens Co., Prairie, MN), were the strongest diffusers (designated LP by the manufacturer) used in our previous studies of form-deprivation myopia.34 Diffusers reduced the contrast sensitivity of adult humans by more than 1 log unit for spatial frequencies of 0.125 cyc/deg, with a resultant cutoff spatial frequency near 1 cyc/deg.34 The diffuser-rearing procedures were initiated at 22 ± 2 days of age, and the monkeys wore the diffusers continuously until 163 ± 17 days of age. Control data on peripheral refractions were obtained from six infant monkeys reared with normal unrestricted vision. Comparison data on central refractive development were available from 31 monkeys reared with unrestricted vision. Data for 25 of these control monkeys have been previously reported.19,26,33–37

Ocular Biometry

Biometry measurements were collected at the start of the diffuser-rearing period and then every 2 to 4 weeks throughout the treatment period. Basic details of the biometric measurements have been described elsewhere.26,33,38 Briefly, to obtain the ocular measurements, the monkeys were anesthetized with intramuscular injections of ketamine hydrochloride (15–20 mg/kg) and acepromazine maleate (0.15–0.2 mg/kg), and cycloplegia was produced with topically administered 1% tropicamide.

Refractive status of each eye was determined independently by two experienced investigators by streak retinoscopy and then was averaged and specified as the spherical-equivalent, spectacle-plane refractive correction. Detailed procedures for peripheral retinoscopy have been described elsewhere.26 In brief, refractive errors were measured along the pupillary axis (the “central” refraction) and at 15° intervals along the horizontal meridian to eccentricities of 45°.

Ocular axial dimensions were measured by A-scan ultrasonography implemented with either a 7-MHz transducer (Image 2000; Mentor, Norwell, MA) or a 12-MHz transducer (OTI Scan 1000; OTI Ophthalmic Technologies, Inc., ON, Canada). Corneal curvature was measured with a hand-held keratometer (Alcon Auto-keratometer; Alcon Systems Inc., St. Louis, MO) or a video topographer (EyeSys 2000; EyeSys Technologies Inc., Houston, TX), or both. Each instrument provided repeatable and comparable measures of central corneal curvature in infant monkeys.38 The video topographer also provided measures of the shape of the peripheral cornea.

Magnetic Resonance Imaging

Near the end of the diffuser-rearing period (approximately 150 days of age), magnetic resonance imaging (MRI) was performed on 11 representative animals with a horizontal bore scanner (7T Bruker Biospec USR 70/30; Bruker, Karlsruhe, Germany). A 155-mm inner-diameter volume coil supplied by Bruker was used for radiofrequency transmission and signal reception.

To obtain the MRI scans, the monkeys were initially anesthetized with 4% to 5% isoflurane in an air/oxygen mixture (7:3). To stabilize the animals during the recording session, the monkeys were intubated and maintained on 2% isoflurane gas anesthesia administered through an anesthesia system (ventilator, Inspira asv [Harvard Apparatus, Holliston, MA]; vaporizer, VMS Anesthesia Machine [MDS Matrix, Orchard Park, NY]). Body temperature was kept at

36.5C° ± 1C° with a feedback-controlled warm air system (SA Instruments, Stony Brook, NY). Throughout the MRI procedures, respiration rate and rectal temperature were measured using a small-animal monitoring system (SA Instruments). Blood oxygen saturation and heart rate were monitored with an MRI-compatible pulse oximeter (NONIN, Plymouth, MN). The monkey's head was fixed on a custom-designed head holder, and petrolatum ophthalmic ointment was applied topically to prevent the ocular surfaces from drying during MRI scans.

The initial tripilot scan was used to localize the positions of the monkey's eyes. Magnetic field homogeneity was then optimized using localized shimming with a point-resolved spectroscopy procedure. Anatomic images were acquired with a three-dimensional (3D)-rapid acquisition paradigm with a relaxation enhancement sequence. Image signals were enhanced with a 3D method by which all scan slices were acquired simultaneously, in contrast to conventional 2D methods by which scan slices are acquired separately. Scan parameters of the axial images were as follows: field of view (FOV) varied from 50 × 50 × 20 mm to 50 × 50 × 30 mm, depending on eye size; acquisition matrix varied correspondingly from 256 × 256 × 40 to 256 × 256 × 60 to ensure that a slice thickness of 0.5 mm was maintained. Spatial resolution of the axial images was 0.195 × 0.195 × 0.5 mm. T_2-weighted images were obtained with long repetition (TR, 1500 ms) and effective echo times (TE, 96 ms) to enhance the contrast between the fluids and tissues of the eye. Average scan time per session was approximately 40 minutes.

Acquired axial MR images were reconstructed with the use of in-house software developed with numerical computing environment and programming language (MATLAB; Mathworks, Natick, MA), which allowed the MR images to be viewed from axial, sagittal, and coronal orientations. The software interpolated between the axial image slices to produce uniform resolution of 0.195 mm in the 3D matrix. To ensure that measurements of the ocular dimensions were obtained from the appropriate image plane, the 3D volumes were rotated so that in the sagittal orientation, the line connecting the equatorial poles of the lens was vertical. The rotation angle was in the range of 4° to 29°. A Canny edge detection algorithm was applied to the horizontal plane of the rotated volumes to determine the boundaries between ocular structures. The approximate optical axis was defined as the perpendicular through the midpoint of the line connecting the equatorial poles of the lens. Lens thickness was determined as the distance along this axis from the anterior to the posterior lens surface. The horizontal image slice that contained the greatest lens thickness in the interpolated stack was used for all further measurements. The intersection of the presumed optical axis and the posterior lens surface was considered the approximate position of the second nodal point.36 The primary measure of interest was the vitreous chamber depth, which was defined as the distance between the approximate position of the second nodal point and the retina. Vitreous chamber depth was determined as a function of eccentricity from 45° nasally to 45° temporally in 15° intervals along the horizontal meridian. To assess the overall shape of the globe, we also measured the eye's axial length and the equatorial diameter in the horizontal plane. Axial length was defined as the distance from the anterior corneal surface to the retina along the presumed optical axis. Equatorial diameter was defined as the greatest distance between the nasal and the temporal retinas measured along a line perpendicular to the presumed optical axis.

Statistical Analysis

Mixed-design, repeated-measures ANOVA (SuperANOVA; Abacus Concepts, Inc., Berkeley, CA) and multiple comparisons were used to determine whether there were differences in refractive error as a function of eccentricity or differences in the patterns of peripheral refraction between subject groups, and to compare the symmetry of refractive errors and vitreous chamber depths between nasal and temporal visual fields along the horizontal meridians. Probability values were adjusted with the Geisser-Greenhouse correction. Two-sample *t*-tests were used to compare central refractions and individual ocular components between treated and control

monkeys. Paired *t*-tests were used to compare refractive errors and individual ocular components between the treated and fellow eyes of the diffuser-reared monkeys.

Results

At ages corresponding to the start of the treatment period, control monkeys exhibited moderate degrees of hyperopia along the pupillary axis (Fig. 1A; right eye average, +4.08 ± 2.06 D). On average (open circles), peripheral refractions in the temporal field tended to be similar to the central refraction or slightly more hyperopic. In contrast, as previously reported,26 peripheral refractions in the near nasal fields (i.e., the 15° and 30° eccentricities) of the control monkeys were consistently less hyperopic than the central refractions. However, during the subsequent rapid period of emmetropization, there was a reduction in the average central (right eye, +2.33 ± 0.41 D) and peripheral refractions, and the pattern of peripheral refractions became more symmetrical across the horizontal meridian, with most eyes showing small amounts of relative myopia in the temporal and nasal fields (Fig. 1B). At ages corresponding to the end of the treatment period, the average refractive errors for the left and right eyes were well matched centrally and peripherally (Fig. 1C). The average degree of central anisometropia was 0.16 ± 0.12 D, and the range of central anisometropia was +0.31 to –0.25 D (right eye – left eye).

Monocular form deprivation consistently disrupted the emmetropization process, disturbing the interocular balance in refractive errors and typically producing axial myopia in the treated eyes. Figure 2A shows the interocular differences in central refractive error plotted as a function of age for individual form-deprived (filled symbols) and control (thin lines) monkeys. At the start of the treatment period, all form-deprived monkeys had similar hyperopic central refractive errors in both eyes (right eye, +4.06 ± 1.26 D; left eye, +4.23 ± 1.32 D; $T = –1.91$; $P = 0.09$). However, after 2 to 4 weeks of form deprivation, most treated animals demonstrated anisometropia that was outside the control range. Thereafter, the degree of anisometropia typically increased over time. At the end of the lens-rearing period, interocular differences in central refraction varied from +2.69 to –10.31 D (treated eye – fellow eye), and the average degree of anisometropia (4.62 ± 3.22 D) was significantly larger than that observed in control monkeys ($T = –4.38$; $P = 0.002$). The form-deprivation regimen produced relative myopic errors in the treated eyes of most animals; 8 of the 10 treated monkeys exhibited myopic anisometropia that was outside the control range. For one form-deprived animal (MKY ADA 337), the degree of anisometropia was within the control range, and in another treated animal (MKY AMO 345), relative hyperopia developed in the treated eye.

As illustrated in Figure 2B, the degree of central anisometropia in the treated monkeys was highly correlated with interocular differences in vitreous chamber depth ($r^2 = 0.92$; $P < 0.0001$). Every 1-mm interocular difference in vitreous chamber depth resulted in approximately 5.1 D anisometropia. Interocular differences in corneal power also contributed to the observed anisometropia. On average, central corneas of the treated eyes were 0.70 D steeper than the central corneas of their fellow eyes (treated eyes, +55.62 D; fellow eyes, 54.92 D; $T = 3.48$; $P = 0.007$), but interocular differences in corneal asphericity were not consistent, as assessed by topographic Q values (treated eyes, –0.07 ± 0.12; fellow eyes, –0.07 ± 0.08; $T = 0.21$; $P = 0.84$). Alterations in the lens did not appear to contribute to the vision-induced alterations in refractive error. At the end of the treatment period, there were no interocular differences in lens thickness between the treated and fellow eyes (treated eyes, 3.61 ± 0.15 mm; fellow eyes, 3.62 ± 0.15 mm; $T = –1.78$; $P = 0.11$). Even when the analysis of lens thickness was restricted to animals with large myopic anisometropia (>2.0 D), there were no significant differences in lens thickness ($T = –1.34$; $P = 0.23$).

Form deprivation also altered the patterns of peripheral refraction in the treated monkeys. Figure 3 compares the refractive errors obtained along the horizontal meridian at the end of

the treatment period for the fellow (open symbols) and treated (filled symbols) eyes of the diffuser-reared monkeys with those for age-matched control monkeys. The cross-hatched area represents ±2 SD from the mean refractions for the right eyes of the control monkeys. For seven of the treated monkeys, the refractive errors for the fellow eyes were very near or within 2 SD of the mean refractions for the control monkeys at all eccentricities. For the other three treated monkeys (Figs. 3B, C, F), the fellow eyes exhibited higher than normal amounts of central hyperopia, and the pattern of peripheral refractions was more variable, but in each case the degree of relative myopia in the nasal field was greater than that observed in any control animal.

Treated eyes showed a wide range of central refractive errors. Moreover, 9 of 10 treated eyes exhibited altered patterns of peripheral refractions. The six animals with central refractive errors below (i.e., greater myopia) the control range exhibited qualitatively similar patterns of peripheral refractions in their treated eyes (Figs. 3E–J). For these six animals, the greatest departures from normal were in the central field, and the degree of myopia decreased with eccentricity in both the nasal and the temporal fields. In other words, compared with their central refractions, these six monkeys manifested relative peripheral hyperopia. Although the central refractive error for the treated eye of MKY OTH 300 (Fig. 3C) was within the control range, the central refractive error of the treated eye was 3.50 D less hyperopic/more myopic than that for its fellow eye, and the pattern of peripheral refraction in the treated eye was qualitatively similar to that of the six monkeys with myopia. This animal also showed relative peripheral hyperopia in the nasal and the temporal fields that increased in magnitude with eccentricity. Two diffuser-reared monkeys had central refractive errors in the treated eyes that were more hyperopic in the than control eyes. For MKY AMO 345 (Fig. 3A), the degree of hyperopia decreased with eccentricity in the nasal and the temporal fields, resulting in relative peripheral myopia. For MKY ALI 338 (Fig. 3B), the decrease in hyperopia and the concomitant relative peripheral myopia was only observed in the nasal field. MKY ADA 337 (Fig. 3D) was the only diffuser-reared monkey that had central and peripheral refractions in the treated eye that were similar to those in its fellow eye and within the control range at all horizontal eccentricities. The pattern of peripheral refraction in the treated eye of this monkey was indistinguishable from that of control monkeys.

Plots of the relative peripheral refractive errors illustrate how form deprivation altered the pattern of peripheral refraction. In Figure 4 (left), the relative peripheral refractive errors (peripheral – central ametropia) measured at the end of the treatment period are plotted as a function of eccentricity for individual diffuser-reared monkeys. The cross-hatched area represents ±2 SD from the mean relative peripheral refractive errors for the control monkeys. Because accommodation is controlled by the central retina, these plots provide an indication of the effective peripheral refractive error that exists when the eye fixates a given plane in space or when the central refractive error is optically corrected for infinity.

The general pattern of peripheral refractive errors was similar for all eight of the diffuser-reared monkeys with central myopic anisometropia (i.e., the treated eye's central refraction was more myopic than that for the fellow eye). In each of these treated monkeys (filled symbols), the relative peripheral refractions were generally more hyperopic in the periphery; the degree of relative hyperopia increased with eccentricity and was outside the ±2 SD control range at most eccentricities, particularly in the temporal field. MKY AMO 345 (open triangles) was the only monkey to exhibit central hyperopic anisometropia, and it was also the only monkey to consistently show relative peripheral myopia.

Magnitudes of the relative peripheral refractive errors were correlated with the central refractive errors. In the smaller plots to the right in Figure 4, the magnitudes of the relative peripheral refractions are plotted as a function of the central ametropia for each peripheral field eccentricity. Regression analyses confirmed that for the 30° and 45° eccentricities in the nasal

field and at all the temporal field eccentricities, the greater the degree of central form-deprivation myopia, the greater the degree of relative peripheral hyperopia ($r^2 = 0.50 – 0.76$; $P < 0.002$).

Figure 5, which illustrates the longitudinal changes in peripheral refractions for the fellow (open symbols) and treated (filled symbols) eyes for five representative monkeys, shows how the altered patterns of peripheral refraction developed. The animals included in Figure 5 were selected to illustrate the range of central ametropia in the treated eyes (+5.81 to –8.25 D) and to illustrate the early changes in peripheral refractions. The leftmost and rightmost plots for each animal show the refractions at the onset and end of the diffuser-rearing period, respectively. At the start of the rearing period, all the treated monkeys exhibited moderate hyperopic central refractions, and the patterns of peripheral refractions were well matched in both eyes of each animal and were similar to those found in control monkeys. The fellow eyes of most animals exhibited emmetropization in both the central and peripheral fields. Specifically, there were usually systematic reductions in central refractive error to levels of approximately +2.00 to +3.00 D of hyperopia. However, as previously observed in monocularly form-deprived monkeys, there were some clear exceptions.[34,35,39,40] For example, after initial reductions in hyperopia during the first 29 days of lens wear, the fellow eye of MKY KWY 365 (fourth row) developed larger than normal amounts of central hyperopia.

As illustrated by the representative animals shown in the lower four rows of Figure 5, the degree of form-deprivation myopia generally increased with time. However, because the rate of refractive-error changes varied with eccentricity, the overall pattern of peripheral refractions also changed over time. Specifically, the degree of myopic change decreased with eccentricity. Consequently, in the eyes with central form-deprivation myopia, the magnitude of relative peripheral hyperopia increased over time with eccentricity in the nasal and the temporal fields.

The top row of Figure 5 shows the data for the diffuser-reared monkey (MKY AMO 345) in which central hyperopia developed in response to form deprivation. This monkey also showed systematic alterations in the pattern of peripheral refraction during the treatment period. In particular, the peripheral refractions became less hyperopic/more myopic than the central refractive error over time, especially in the temporal field.

Longitudinal data in Figure 5 also demonstrate that the alterations in central refraction and the pattern of peripheral refractive errors were apparent shortly after the onset of form deprivation. Specifically, all the treated monkeys in which form-deprivation myopia was exhibited demonstrated apparent alterations in peripheral refractions at the first measurement session after the onset of diffuser wear (Fig. 5, second column). For example, at the first measurement after treatment onset, there were differences in the pattern of refractions between the fellow eyes and treated eyes of all four of the animals represented in the lower four rows of Figure 5. Two of these monkeys (MKY EDG 354 and MKY ALV 343) also showed evidence of central myopia, exhibiting less hyperopic/more myopic refractions in their treated eyes compared to their fellow eyes. However, for MKY HER 361 and MKY KWY 365, central refractions were similar in both eyes, but peripheral refractions were more hyperopic in the treated eyes; in other words, alterations in the pattern of peripheral refraction were the first noticeable treatment effects in some of the form-deprived eyes.

Interocular comparisons between fellow and treated eyes of the diffuser-reared monkeys demonstrated that form deprivation altered the pattern of peripheral refraction very early in the treatment period. Figure 6 shows the normalized interocular difference plots obtained at the first measurement session after the onset of diffuser wear. Specifically, to characterize the interocular differences in the pattern of peripheral refractions, the data for each eye were first normalized to that eye's central refractive error, and then the relative refractive errors for the

fellow eyes were subtracted from those for the treated eyes at each eccentricity. Although the magnitude of the differences between central and peripheral refractions were small, many of the diffuser-reared monkeys (filled symbols) exhibited relative peripheral hyperopic errors that were outside the control range for age-equivalent animals. In particular, all eight of the diffuser-reared animals that eventually developed central myopic anisometropia showed relative hyperopic errors that were outside the control range (thin lines) at many peripheral eccentricities, especially in the temporal field ($F = 36.213$; $P = 0.0018$). Significant differences occurred at the temporal 45° eccentricity ($F = 11.703$; $P = 0.002$) and at the temporal 30° eccentricity ($F = 18.832$; $P = 0.0002$). However, for 5 of 8 treated monkeys with relative peripheral hyperopia in the treated eyes, the degree of central anisometropia was within ±2 SD of the mean for the control monkeys, and the central vitreous chamber depths for the treated eyes of these five diffuser-reared monkeys were equal to or shorter than those for their fellow eyes. In other words, many of the diffuser-reared monkeys exhibited relative peripheral hyperopia in their treated eyes before showing obvious signs of central axial myopia.

MRI was performed on two control monkeys and nine monkeys that experienced form deprivation. Axial length of the eye was measured from the corneal surface to the vitreo-retinal interface along the line that was perpendicular to and bisected the line connecting the equatorial poles of the lens (see Fig. 7). Axial dimensions obtained from the MRI scans compared favorably with axial length data obtained by A-scan ultrasonography. For example, the average vitreous chamber depths determined by ultrasonography and from the magnetic resonance images were, respectively, 10.45 ± 1.00 mm versus 10.55 ± 1.00 mm for the right eyes and 9.95 mm ± 0.56 mm versus 9.97 ± 0.58 mm for the left eyes. Mean differences between the MRI and A-scan measurements were –0.10 ± 0.33 mm and –0.02 ± 0.23 mm for the right and left eyes, respectively, and were not statistically different from zero ($P = 0.33$ and $P = 0.77$, respectively). MRI and A-scan data for the individual eyes were also highly correlated ($r^2 = 0.89$ and 0.85 for the right and left eyes, respectively; $P < 0.0001$). Equatorial diameters in the MR images were measured in the horizontal plane and were defined as the greatest distance between the nasal and temporal retinas along a line that was perpendicular to the axial length projection. Resultant axial lengths and equatorial diameters for both eyes of each animal are presented in Table 1.

Comparisons of the axial lengths and equatorial diameters for the fellow and treated eyes showed that form deprivation altered the overall shape of the globe. For instance, even though corneal height was included in the MRI axial length measures, the fellow eyes of 8 of 9 diffuser-reared monkeys (average equatorial diameter, 17.00 mm; average axial length, 16.28 mm; $T = –4.0$; $P = 0.004$) and both eyes of the control animals had longer equatorial diameters than axial lengths (i.e., the fellow eyes of the diffuser-reared monkeys, as in control monkeys, were oblate). On the other hand, the treated eyes of the diffuser-reared monkeys that developed relative myopic anisometropia were less oblate/more prolate. In particular, the axial lengths of the treated eyes that developed relative myopic refractive errors were longer than those of their fellow eyes. Specifically, for the seven treated monkeys that underwent MRI and that exhibited more than –0.50 D myopic anisometropia, the average axial length was 16.99 ± 1.09 mm for the treated eyes and 16.15 ± 0.58 mm for the fellow eyes ($T = 3.14$; $P = 0.02$). However, the equatorial diameters of the treated and fellow eyes of these animals were not significantly different (17.17 ± 0.98 mm vs. 16.83 ± 0.77 mm; $T = 1.99$; $P = 0.09$). In contrast to their fellow eyes, equatorial diameters were not significantly greater than axial lengths in treated eyes ($T = –0.91$; $P = 0.397$). As a result, the ratios of axial length to equatorial diameter in the treated eyes were significantly greater (less oblate) than those for the fellow eyes (0.99 ± 0.03 vs. 0.96 ± 0.02; $T = 3.83$; $P = 0.009$).

MRI also demonstrated that the alterations in peripheral refraction resulted from eccentricity-dependent changes in vitreous chamber depth and the shape of the posterior globe. The left

column in Figure 8 shows the MRI scans obtained at the end of the diffuser-rearing period for the treated (left) and fellow (right) eyes of five representative form-deprived monkeys. In the middle column, the vitreous chamber depths determined from the MR images (see Fig. 7) are plotted as a function of retinal eccentricity for the treated (filled symbols) and fellow (open symbols) eyes. The graphs in the right column show the interocular differences in refractive error (open symbols, left ordinate) and vitreous chamber depth (filled symbols, right ordinate) plotted as a function of visual field eccentricity. In the right plots, negative numbers on the *y*-axis indicate that the treated eye was more myopic or had a longer vitreous chamber than its fellow eye.

As expected, the MR images revealed differences in central vitreous chamber depth between the treated and fellow eyes of the diffuser-reared monkeys. For MKY AMO 345 (top row), the only diffuser-reared monkey that developed hyperopic anisometropia, the central vitreous chamber depth was shorter in the treated eye. The treated eyes of all the monkeys with myopic anisometropia had longer central vitreous chambers than their fellow eyes (e.g., lower four rows in Fig. 8). In the animals with large amounts of form-deprivation myopia (e.g., bottom two rows), simple inspection of the MR images revealed that the vitreous chambers of the treated eyes were larger than those of the fellow eyes.

More important, the MR images revealed interocular differences in the shapes of the posterior globe that were correlated with the interocular differences in peripheral refraction. For the control and fellow eyes, vitreous chamber depth was consistently greater in the temporal retina ($F = 7.191$; $P = 0.02$). For most of the fellow and control eyes, however, the differences in vitreous chamber depth between the central and peripheral eccentricities were less than 0.5 mm (i.e., vitreous chamber depth was relatively constant across the central 45° of retina). Only MKY OTH 300 (second row), the monkey that showed a high degree of central hyperopia and substantial nasal-temporal asymmetries in refractive error in its fellow eye, demonstrated larger variations in vitreous chamber depth. In contrast, all the treated eyes showed substantial central versus peripheral differences in vitreous chamber depth along the horizontal meridian. As a consequence, the interocular differences in vitreous chamber depth varied with eccentricity.

Moreover, comparisons between interocular differences in refraction and vitreous chamber depth in individual animals (Fig. 8, right column) showed a close correspondence between the changes in peripheral refraction and eye shape. In particular, the similarities between these functions showed that the vitreous chamber depths of the treated eyes were relatively longer at eccentricities where the treated eyes were relatively more myopic and visa versa. For example, for MKY AMO 345 (Fig. 8, top row), the monkey with hyperopic anisometropia, the vitreous chamber was shorter and the relative refractions were more hyperopic in the treated eye at all eccentricities. On the other hand, as captured in the interocular difference plots for the monkeys with form-deprivation myopia (lower 4 rows in Fig. 8), the degree of relative myopia and relative axial elongation were greatest in the central retinas/fields and decreased in a parallel fashion with eccentricity in the nasal and temporal retinas/fields. As illustrated in Figure 9, there was a strong correlation between interocular differences in peripheral refractive error and vitreous chamber depth ($r^2 = 0.87$; $P < 0.0001$) for the combined data set. As observed for central refractive errors and A-scan axial lengths (Fig. 2), a 1-mm difference in peripheral vitreous chamber depths corresponded to approximately a 5-D difference in peripheral refractive error.

Discussion

Changes in the development of central refractive error produced by our diffuser-rearing regimen were similar to those reported previously for form-deprived infant monkeys. Specifically, in most animals, the treated eyes exhibited faster vitreous chamber elongation

rates and became less hyperopic/more myopic than their fellow nontreated eyes.20,34,35,41–43 There was substantial variability in the degree of relative form-deprivation myopia between animals, with a small number of treated eyes showing either no change in refractive error or relative hyperopic changes.34,35,41,43 In addition, a small number of form-deprived monkeys exhibited alterations in the refractive states of their fellow, nontreated eyes.20,34,35,39 The primary new findings were that form deprivation also altered the pattern of peripheral refractions and the shape of the posterior globe in macaques.

In agreement with our findings, Troilo et al.44 and Totonelly et al. (*IOVS* 2008;49:ARVO E-Abstract 3589) have recently reported that optically induced defocus also alters eye shape and the pattern of peripheral refractions in marmosets. In both species of primates, central axial myopia was associated with relative peripheral hyperopia and a more prolate eye. There were, however, some differences between the vision-induced alterations in peripheral refractions produced in marmosets and macaques. Although the increases in relative hyperopia with eccentricity were relatively symmetrical in the nasal and temporal fields of macaques, the relative peripheral hyperopia was restricted to the temporal field in marmosets.

Patterns of peripheral refraction in our control and form-deprived monkeys were similar in several respects to those found in children and adults with naturally occurring refractive errors. For example, the patterns of peripheral refraction in humans and monkeys vary in the same manner with the central refractive state. As in most humans with emmetropia, after the rapid phase of emmetropization, our control monkeys (animals that presumably had the optimal refractive states for their species) showed small amounts of relative myopia in the near periphery.26 In our diffuser-reared monkeys with myopia, as in most humans with myopia, the treated eyes exhibited relative hyperopic shifts in the horizontal periphery4,5,21; the degree of relative peripheral hyperopia increased with the degree of central myopia,22,23 and there was evidence that the relative peripheral hyperopia often developed before the onset of central axial myopia.15,17 In addition, as in many humans with hyperopia, the diffuser-reared monkey with absolute and relative (with respect to the fellow eye) central hyperopic errors in the treated eye also demonstrated relative myopic shifts in the periphery. In general, the correlations between central and peripheral refractive errors were more consistent in monkeys than in humans,1 probably because our monkey population was more homogeneous in terms of age and visual experience than human subject populations and because our monocular treatment strategy allowed interocular comparisons.

The overall shape of the control and fellow eyes and the ocular changes associated with alterations in the peripheral refractions of our treated myopic monkeys were also qualitatively similar to those observed in humans. Many techniques—x-ray tomography,45 B-scan ultrasonography,46 computed tomography,47 optical coherence reflectometry,48 MRI23–25,49—have been used to compare eye shape and refractive error in humans. Although there is substantial variability in eye shape between subjects, between studies, and within a given refractive error group, there is general agreement that the eyes of humans with emmetropia are typically oblate and that the eyes of those with myopia have larger equatorial (horizontal) diameters and much longer axial lengths. As a consequence, the posterior globes of myopic eyes are less oblate/more prolate than of emmetropic eyes. Our interocular comparisons of axial length and equatorial diameter and the measurements of vitreous chamber depth along the horizontal meridian show that the myopic eyes of our treated monkeys exhibited longer axial lengths and steeper retinal contours. In other words, myopic eyes were less oblate/more prolate than their fellow eyes. In particular, the results from our form-deprived monkeys are in good agreement with the eye shape model of Atchison et al.24 for the average myopic human eye.

The close correspondence between interocular differences in vitreous chamber depth and interocular differences in refractive error observed in individual form-deprived monkeys (Figs. 8, 9) is important because it demonstrates that the vision-induced alterations in the peripheral refractions of our treated monkeys chiefly reflected local changes in retinal curvature. There have been few attempts in humans to directly compare eye shape and peripheral refractions in the same eye. However, Schmid,48 with the use of optical coherence reflectometry to measure eye length in humans, also found a significant correlation between relative peripheral eye length (changes in eye length as a function of eccentricity) and relative peripheral refraction, particularly in the horizontal meridian. In other words, in monkeys and humans, the pattern of relative peripheral refraction is correlated with retinal curvature, which reinforces the idea that retinal curvature largely determines the overall pattern of peripheral refractive errors.

The potential role of peripheral refractive errors, specifically relative peripheral hyperopia, as a risk factor for the onset and progression of myopia is dependent on when the peripheral errors are manifest. There are some discrepancies between studies regarding the temporal relationship between the onset of peripheral and central refractive errors in humans. In a longitudinal study of young adults undergoing pilot training, Hoogerheide et al.15 found that relative peripheral hyperopia precedes adult-onset myopia in emmetropic eyes. No data on axial lengths were reported. However, given that the subjects were adults and that the refractive-error measures were obtained before the onset of the behavior that presumably triggered the onset of myopia, it is reasonable to assume that the peripheral errors also preceded central axial elongation. On the other hand, although Mutti et al.17 also found that peripheral hyperopia precedes the onset of central myopia by several years (though the lead time reflects, in part, their conservative criteria for myopia onset), they reported that peripheral refractive errors were secondary to changes in central axial length (i.e., the onset of axial elongation started before the onset of peripheral hyperopia). This pattern of results argues against a causal relationship between peripheral hyperopia and axial myopia.

Our observations in monkeys demonstrate that alterations in peripheral refraction can occur before any detectable changes in axial length or central refractive error. However, because our diffuser lenses severely degraded the retinal image, it seems unlikely that any resultant peripheral hyperopic defocus contributed to the observed axial myopia in our treated monkeys. Consequently, our results do not necessarily support a causal relationship between peripheral hyperopia and central myopia. It is possible that the peripheral hyperopia found in our infant monkeys reflects early programmatic changes in eye shape that are associated with the process of axial elongation; in other words, peripheral hyperopia may represent the first detectable change in response to any myopiagenic visual stimulus. Similarly, the peripheral myopia exhibited by the treated monkey with central hyperopia in response to form deprivation and the variations in the patterns of peripheral refractions with central refractive errors in 3-week-old control monkeys appeared to reflect differences in eye shape associated with absolute differences in axial length and preprogrammed genetic growth processes.26 Thus, none of our observations in monkeys necessarily provides direct support for a causal relationship between peripheral and central refractions. However, regardless of whether peripheral hyperopia is a concomitant change that occurs during axial elongation or whether peripheral hyperopia develops independently, given that selective peripheral hyperopic defocus can produce axial myopia in infant monkeys (Smith EL III, et al. *IOVS* 2007;48:ARVO E-Abstract 1533), it is likely that the presence of peripheral hyperopia will subsequently promote myopic progression and increase the severity of myopia. In this respect, the presence of peripheral hyperopia may be helpful in identifying those who are likely to become myopic or to exhibit myopic progression in the future.15,17,18

Why does form deprivation promote a selective change in eye shape rather than an overall expansion of the posterior globe? Various potential factors may influence eye shape during

growth, many of which are essentially mechanical in nature. For example, it has been argued that anatomic constraints imposed by the orbit and/or extraocular muscles allow for axial elongation but restrict equatorial expansion.21,23 In marmosets, in which the eyes are positioned very close to the medial orbital wall, the marked nasal-temporal asymmetries in vitreous chamber depth found in myopic eyes appear to reflect physical constraints imposed by the orbit (Totonelly KC, et al. *IOVS* 2008;49:ARVO E-Abstract 3589). Inspection of the MRI scans for the treated monkeys shows that, as in humans, the medial and lateral orbital walls and the anterior portions of the rectus muscles are closely aligned with the equator of the eye, whereas there is substantial space between the posterior pole and the apex of the orbit. Thus, mechanical factors could contribute to the shape changes found in our myopic monkeys.

Based on differences in lens thickness observed in some studies of children with myopia and children without myopia, it has been hypothesized that mechanical tension originating in the lens could also physically constrain equatorial expansion during growth, resulting in a more prolate eye.16,17 However, there were no signs of lens thinning in the treated eyes of our diffuser-reared monkeys. Moreover, in an analysis of a large number of monkeys with experimentally induced ametropia, we did not find significant differences in any lens parameters (thickness, surface curvature, or equivalent power) among hyperopic, emmetropic, and myopic eyes (unpublished data). Thus, it appears that the relative prolate changes in ocular shape associated with myopia can occur without any signs of lens involvement.

Regional variations in the vision-dependent biological processes that regulate eye growth could also contribute to changes in eye shape during axial elongation. As in chickens50–52 and tree shrews,53 hemiretinal form deprivation produces regionally selective changes in peripheral refraction and vitreous chamber depth in infant monkeys.54 These experiments indicate that the effects of vision on refractive development in primates are dominated by local retinal mechanisms that integrate visual signals in a spatially restricted manner and exert their influence selectively on the subjacent sclera. Although little is known about the spatial summation characteristics of these local retinal mechanisms, regional anisotropy in the number, density and/or sensitivity of these mechanisms could alter the shape of the globe in response to a visual growth signal. Details concerning the retinal components of the signal cascade associated with these local mechanisms are sketchy; however, it is likely that cone photoreceptors are involved in initiating the visual signals that influence ocular growth.55 In this respect, it is well known that the number and density of cones, like those of many, but not all, retinal neuron types, are highest near the posterior pole of the primate eye and decrease with eccentricity. Assuming that the growth-regulating signal strength is related to the density or absolute numbers of retinal neurons, many viewing conditions that promote myopia, in particular full-field form deprivation, would be expected to have their greatest effects near the posterior pole. In agreement with this idea, several observations indicate that form deprivation preferentially affects the composition of the sclera near the posterior pole. For example, in mammals, form deprivation preferentially reduces the scleral synthesis rates of proteoglycans31,56 and glycosaminoglycans57 to a greater degree in the posterior pole than at the equator. The loss of these structural components is thought to alter the biomechanical properties of the extracellular matrix of the sclera, specifically increasing the extensibility of the posterior sclera.58

In many species, axial growth appears to be regulated by visual feedback associated with the effective refractive state of the eye, in essence optical defocus. It is important to recognize that under ordinary viewing conditions, the effects of a given level of optical defocus will vary with eccentricity, especially in primates that have a highly developed fovea. In essence, for a given level of defocus, the optical consequences are likely to be more severe at the fovea and to decrease with eccentricity because the spatial resolving capacities and the sensitivity to blur for most neurons decreases with eccentricity. Consequently, ignoring spatial summation and

neural density issues, experimentally imposed hyperopic optical defocus would be expected to have a greater effect on axial growth near the posterior pole than in the periphery and, it is reasonable to argue, would promote a more prolate eye. Thus, in normal environments, several aspects of the retinal architecture could promote a more prolate shape in myopic eyes. However, it is unlikely that variations in retinal resolving capacity influenced our results. We specifically used severe form deprivation to produce the maximal stimulus for ocular growth at all eccentricities. Consequently, the changes in ocular shape that we observed were probably not caused by eccentricity-dependent variations in spatial resolution and the effective degree of image degradation.

However, because our stimulus for ocular growth should have been effective in the central and peripheral retina, it is important to consider how a peripheral stimulus for growth would affect central axial length. As Seidmann et al.10 discuss, an expansion of the sclera in the periphery would displace the central retina in a posterior direction along the visual axis. In agreement with this idea, we have previously demonstrated that peripheral visual signals can influence central refractive development in young monkeys in a manner that is independent of the nature of central vision.19,20 Given that the biomechanical changes that occur in the sclera during the development of myopia lead to tangential stretching of the sclera, it is possible that central and peripheral visual signals for growth would lead to a relative prolate expansion of the globe such as we observed in our form-deprived eyes.

In infant monkeys emmetropization occurs for central and peripheral refractive errors, which is in agreement with the hypothesis that during refractive development eye shape is regulated to optimize peripheral refractive errors.59–63 Our results from form-deprived monkeys demonstrate that visual experience can disrupt this process and, in addition to producing axial myopia, can alter ocular shape and induce abnormal peripheral refractive errors. Given the similarities between monkey and human eyes,36,37 it is likely that visual experience can also promote the development of central and peripheral refractive errors in humans. In humans, it is not clear what factors lead to the association between peripheral and central refractive errors. Although peripheral hyperopia can produce central axial myopia in primates (Smith EL III, et al. *IOVS* 2007;48:ARVO E-Abstract 1533), results from this study show that the association between peripheral hyperopia and axial myopia is not necessarily causal in nature. Nevertheless, the findings from this study emphasize that to understand the role of vision in normal refractive development and the genesis of common refractive errors, it is important to consider the effects of visual experience on eye shape and on central and peripheral refraction.

Acknowledgments

Supported by National Institutes of Health Grants EY-03611, EY-07551, and RR17205, and by funds from Vision CRC and the UH Foundation.

References

1. Stone RA, Flitcroft DI. Ocular shape and myopia. Ann Acad Med Singapore 2004;33:7–15. [PubMed: 15008555]
2. Ferree CE, Rand G, Hardy C. Refraction for the peripheral field of vision. Arch Ophthalmol 1931;5:717–731.
3. Millodot M, Lamont A. Refraction of the periphery of the eye (letter). J Opt Soc Am 1974;64:110–111. [PubMed: 4813433]
4. Ferree CE, Rand G. Interpretation of refractive conditions in the peripheral field of vision. Arch Ophthalmol 1933;9:925–938.
5. Millodot M. Effect of ametropia on peripheral refraction. Am J Optom Physiol Opt 1981;58:691–695. [PubMed: 7294139]

6. Rempt F, Hoogerheide J, Hoogenboom WP. Peripheral retinoscopy and the skiagram. Ophthalmologica 1971;162:1–10. [PubMed: 5547863]
7. Charman WN, Jennings JAM. Longitudinal changes in peripheral refraction with age. Ophthalmic Physiol Opt 2006;26:447–455. [PubMed: 16918768]
8. Lotmar W, Lotmar T. Peripheral astigmatism in the human eye: experimental data and theoretical model predictions. J Opt Soc Am 1974;64:510–513. [PubMed: 4822573]
9. Gustafsson J, Terenius E, Buchheister J, Unsbo P. Peripheral astigmatism in emmetropic eyes. Ophthalmic Physiol Opt 2001;21:393–400. [PubMed: 11563427]
10. Seidemann A, Schaeffel F, Guirao A, Lopez-Gil N, Artal P. Peripheral refractive errors in myopic, emmetropic, and hyperopic young subjects. J Opt Soc Am A Opt Image Sci Vis 2002;19:2363–2373. [PubMed: 12469730]
11. Ferree CE, Rand G, Hardy C. Refractive asymmetry in the temporal and nasal halves of the visual field. Am J Ophthalmol 1932;15:513–522.
12. Atchison DA, Pritchard N, White SD, Griffiths AM. Influence of age on peripheral refraction. Vision Res 2005;45:715–720. [PubMed: 15639498]
13. Artal P, Derrington AM, Colombo E. Refraction, aliasing, and the absence of motion reversals in peripheral vision. Vision Res 1995;35:939–947. [PubMed: 7762151]
14. Wang YZ, Thibos LN, Bradley A. Effects of refractive error on detection acuity and resolution acuity in peripheral vision. Invest Ophthalmol Vis Sci 1997;38:2134–2143. [PubMed: 9331277]
15. Hoogerheide J, Rempt F, Hoogenboom WP. Acquired myopia in young pilots. Ophthalmologica 1971;163:209–215. [PubMed: 5127164]
16. Mutti DO, Zadnik K, Hayes JR, Mitchell GL, Jones LA, Moeschberger ML. Axial length and ocular shape before and after the onset of myopia. Optom Vision Sci 2004;12S:24.
17. Mutti DO, Hayes JR, Mitchell GL, et al. Refractive error, axial length, and relative peripheral refractive error before and after the onset of myopia. Invest Ophthalmol Vis Sci 2007;48:2510–2519. [PubMed: 17525178]
18. Schmid G. Retinal steepness vs. myopic shift in children. Optom Vision Sci 2004;12S:23.
19. Smith EL III, Kee C-S, Ramamirtham R, Qiao-Grider Y, Hung L-F. Peripheral vision can influence eye growth and refractive development in infant monkeys. Invest Ophthalmol Vis Sci 2005;46:3965–3972. [PubMed: 16249469]
20. Smith EL III, Ramamirtham R, Qiao-Grider Y, et al. Effects of foveal ablation on emmetropization and form-deprivation myopia. Invest Ophthalmol Vis Sci 2007;48:3914–3922. [PubMed: 17724167]
21. Mutti DO, Sholtz RI, Friedman NE, Zadnik K. Peripheral refraction and ocular shape in children. Invest Ophthalmol Vis Sci 2000;41:1022–1030. [PubMed: 10752937]
22. Logan NS, Gilmartin B, Wildsoet CF, Dunne MC. Posterior retinal contour in adult human anisomyopia. Invest Ophthalmol Vis Sci 2004;45:2152–2162. [PubMed: 15223789]
23. Atchison DA, Jones CE, Schmid KL, et al. Eye shape in emmetropia and myopia. Invest Ophthalmol Vis Sci 2004;45:3380–3386. [PubMed: 15452039]
24. Atchison DA, Pritchard N, Schmid KL, Scott DH, Jones CE, Pope JM. Shape of the retinal surface in emmetropia and myopia. Invest Ophthalmol Vis Sci 2005;46:2698–2707. [PubMed: 16043841]
25. Singh KD, Logan NS, Gilmartin B. Three-dimensional modeling of the human eye based on magnetic resonance imaging. Invest Ophthalmol Vis Sci 2006;47:2272–2279. [PubMed: 16723434]
26. Hung LF, Ramamirtham R, Huang J, Qiao-Grider Y, Smith EL 3rd. Peripheral refraction in normal infant rhesus monkeys. Invest Ophthalmol Vis Sci 2008;49:3747–3757. [PubMed: 18487366]
27. Greene PR. Mechanical considerations in myopia: relative effects of accommodation, convergence, intraocular pressure, and the extraocular muscles. Am J Optom Physiol Opt 1980;57:902–914. [PubMed: 7223834]
28. van Alphen GW. Choroidal stress and emmetropization. Vision Res 1986;26:723–734. [PubMed: 3750852]
29. Battaglioli JL, Kamm RD. Measurements of the compressive properties of scleral tissue. Invest Ophthalmol Vis Sci 1984;25:59–65. [PubMed: 6698732]
30. Walker TW, Mutti DO. The effect of accommodation on ocular shape. Optom Vis Sci 2002;79:424–430. [PubMed: 12137396]

31. Rada JA, Nickla DL, Troilo D. Decreased proteoglycan synthesis associated with form deprivation myopia in mature primate eyes. Invest Ophthalmol Vis Sci 2000;41:2050–2058. [PubMed: 10892842]
32. McBrien NA, Cottriall CL, Annies R. Retinal acetylcholine content in normal and myopic eyes: a role in ocular growth control? Vis Neurosci 2001;18:571–580. [PubMed: 11829303]
33. Smith EL III, Hung L-F. The role of optical defocus in regulating refractive development in infant monkeys. Vision Res 1999;39:1415–1435. [PubMed: 10343811]
34. Smith EL III, Hung L-F. Form-deprivation myopia in monkeys is a graded phenomenon. Vision Res 2000;40:371–381. [PubMed: 10820617]
35. Smith EL III, Hung L-F, Kee C-S, Qiao Y. Effects of brief periods of unrestricted vision on the development of form-deprivation myopia in monkeys. Invest Ophthalmol Vis Sci 2002;43:291–299. [PubMed: 11818369]
36. Qiao-Grider Y, Hung LF, Kee CS, Ramamirtham R, Smith EL 3rd. Normal ocular development in young rhesus monkeys (*Macaca mulatta*). Vision Res 2007;47:1424–1444. [PubMed: 17416396]
37. Qiao-Grider Y, Hung L-F, Kee C-S, Ramamirtham R, Smith EL III. A comparison of refractive development between two subspecies of infant rhesus monkeys (*Macaca mulatta*). Vision Res 2007;47:1668–1681. [PubMed: 17442365]
38. Kee C-S, Hung L-F, Qiao Y, Habib A, Smith EL III. Prevalence of astigmatism in infant monkeys. Vision Res 2002;42:1349–1359. [PubMed: 12044741]
39. Bradley DV, Fernandes A, Boothe RG. The refractive development of untreated eyes of rhesus monkeys varies according to the treatment received by their fellow eyes. Vision Res 1999;39:1749–1757. [PubMed: 10343866]
40. Bradley DV, Fernandes A, Lynn M, Tigges M, Boothe RG. Emmetropization in the rhesus monkey (*Macaca mulatta*): birth to young adulthood. Invest Ophthalmol Vis Sci 1999;40:214–229. [PubMed: 9888446]
41. Smith EL III, Harwerth RS, Crawford MLJ, von Noorden GK. Observations on the effects of form deprivation on the refractive status of the monkey. Invest Ophthalmol Vis Sci 1987;28:1236–1245. [PubMed: 3610541]
42. Wiesel TN, Raviola E. Myopia and eye enlargement after neonatal lid fusion in monkeys. Nature 1977;266:66–68. [PubMed: 402582]
43. Tigges M, Tigges J, Fernandes A, Eggers HM, Gammon JA. Postnatal axial eye elongation in normal and visually deprived rhesus monkeys. Invest Ophthalmol Vis Sci 1990;31:1035–1046. [PubMed: 2354909]
44. Troilo, D.; Totonelly, KC. Studies of eye shape and peripheral refractive state in marmosets reared with single vision contact lenses.. Presented at: 12th International Myopia Conference; Palm Cove, Australia. July 8–12, 2008;
45. Deller J, O'Connor A, Sorsby A. X-ray measurements of the diameters of the living eye. Proc R Soc Lond B Biol Sci 1947:456–467.
46. Vohra SB, Good PA. Altered globe dimensions of axial myopia as risk factors for penetrating ocular injury during peribulbar anaesthesia. Br J Anaesth 2000;85:242–245. [PubMed: 10992832]
47. Zhou, X-D.; Wang, F-R.; Zhou, S-Z.; Shi, J-S. A computed tomographic study of the relation between ocular axial biometry and refraction.. In: Tokoro, T., editor. Proceedings of the 6th International Conference on Myopia. Springer Tokyo; Kakone-machi, Japan: 1998. p. 112-116.
48. Schmid GF. Axial and peripheral eye length measured with optical low coherence reflectometry. J Biomed Opt 2003;8:655–662. [PubMed: 14563204]
49. Cheng HM, Singh OS, Kwong KK, Xiong J, Woods BT, Brady TJ. Shape of the myopic eye as seen with high-resolution magnetic resonance imaging. Optom Vis Sci 1992;69:698–701. [PubMed: 1437010]
50. Troilo D, Gottlieb MD, Wallman J. Visual deprivation causes myopia in chicks with optic nerve section. Curr Eye Res 1987;6:993–999. [PubMed: 3665562]
51. Hodos W, Kuenzel WJ. Retinal-image degradation produces ocular enlargement in chicks. Invest Ophthalmol Vis Sci 1984;25:652–659. [PubMed: 6724835]
52. Wallman J, Gottlieb MD, Rajaram V, Fugate-Wentzek L. Local retinal regions control local eye growth and myopia. Science 1987;237:73–77. [PubMed: 3603011]

53. Norton TT, Siegwart JT. Local myopia produced by partial visual-field deprivation in tree shrew. Soc Neurosci Abstr 1991;17:558.
54. Smith, EL., III; Huang, J.; Hung, LF. Hemi-retinal form deprivation and refractive development in monkeys.. Presented at: Annual Meeting of the American Academy of Optometry; Anaheim, CA. October 22–25, 2008; Abstract 80005
55. Crewther DP. The role of photoreceptors in the control of refractive state. Prog Retin Eye Res 2000;19:421–457. [PubMed: 10785617]
56. Norton TT, Rada JA. Reduced extracellular matrix in mammalian sclera with induced myopia. Vision Res 1995;35:1271–1281. [PubMed: 7610587]
57. McBrien NA, Lawlor P, Gentle A. Scleral remodeling during the development of and recovery from axial myopia in the tree shrew. Invest Ophthalmol Vis Sci 2000;41:3713–3719. [PubMed: 11053267]
58. Rada JA, Shelton S, Norton TT. The sclera and myopia. Exp Eye Res 2006;82:185–200. [PubMed: 16202407]
59. Hodos W, Erichsen JT. Lower-field myopia in birds: an adaptation that keeps the ground in focus. Vision Res 1990;30:653–657. [PubMed: 2378058]
60. Fitzke FW, Hayes BP, Hodos W, Holden AL, Low JC. Refractive sectors in the visual field of the pigeon eye. J Physiol 1985;369:33–44. [PubMed: 4093886]
61. Miles FA, Wallman J. Local ocular compensation for imposed local refractive error. Vision Res 1990;30:339–349. [PubMed: 2336793]
62. Murphy CJ, Howland M, Howland HC. Raptors lack lower-field myopia. Vision Res 1995;35:1153–1155. [PubMed: 7610576]
63. Schaeffel F, Hagel G, Eikermann J, Collett T. Lower-field myopia and astigmatism in amphibians and chickens. J Opt Soc Am A Opt Image Sci Vis 1994;11:487–495. [PubMed: 8120697]

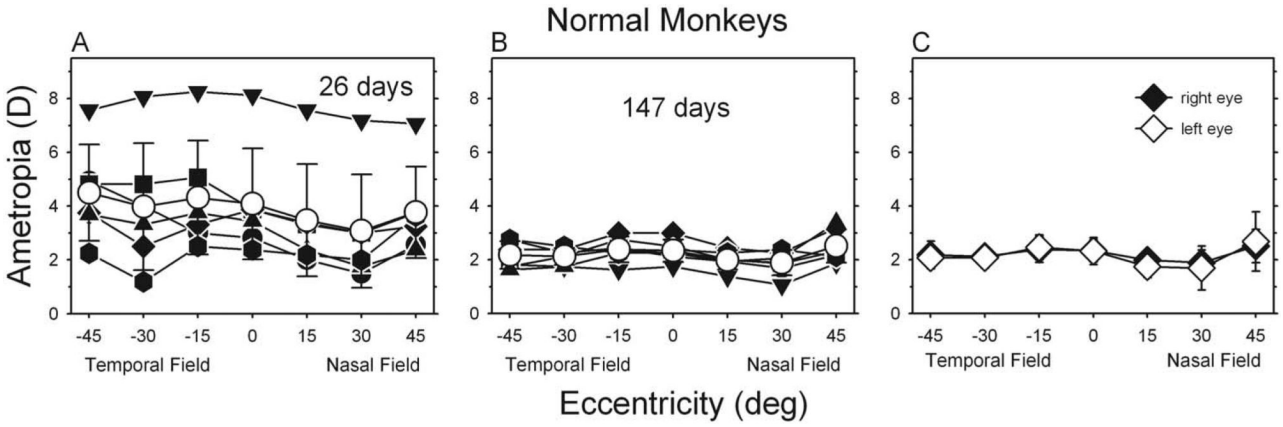

Figure 1.

(**A**, **B**) Spherical-equivalent refractive corrections for the right eyes of control monkeys plotted as a function of visual field eccentricity. Data were obtained at ages corresponding to the start (**A**; average, 26 days of age) and the end (**B**; average, 147 days of age) of the treatment period. *Filled symbols* represent individual monkeys; *open symbols* show group averages (±1 SE). (**C**) Average spherical-equivalent refractive corrections (±1 SE) for the right (*filled symbols*) and left (*open symbols*) eyes for all control monkeys at ages corresponding to the end of the treatment period. Zero eccentricity represents the pupillary axis.

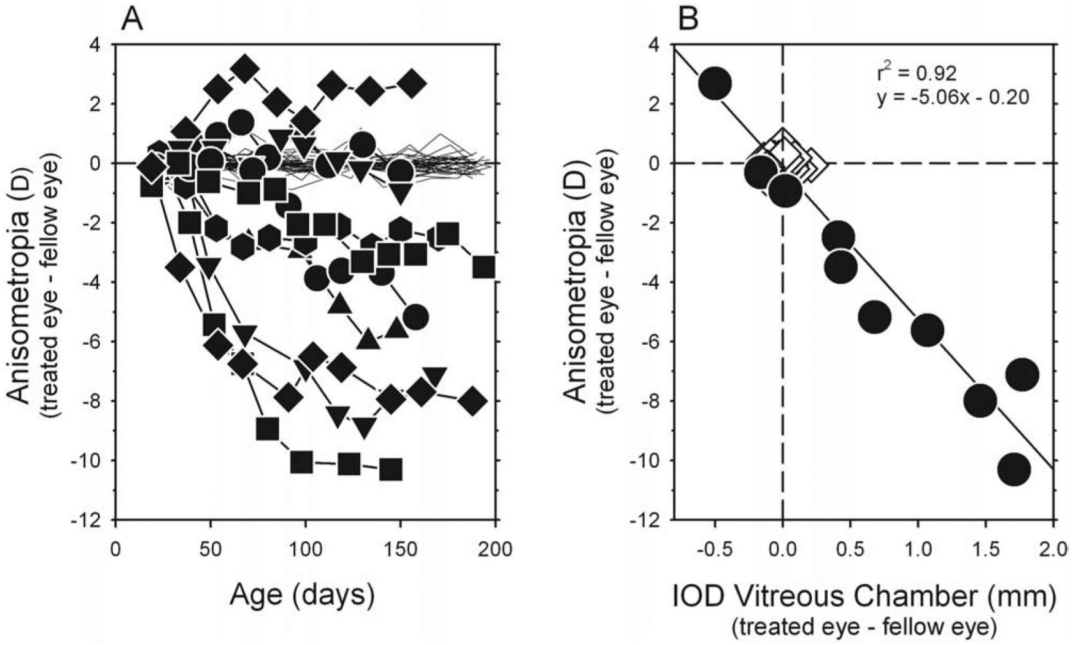

Figure 2.

(**A**) Interocular differences in central refractive error (right or treated eye – left or fellow eye) plotted as a function of age for individual diffuser-reared (*filled symbols*) and control (*thin lines*) monkeys. (**B**) Interocular differences in central spherical-equivalent refractive corrections plotted as a function of the interocular differences in central vitreous chamber depth (right or treated eye – left or fellow eye) for subjects at ages corresponding to the end of the diffuser-rearing period (average = 159 and 163 days of age for control and diffuser-reared monkeys, respectively). *Open diamonds*: control; *filled circles*: diffuser-reared monkeys. *Solid line*: best-fitting regression line.

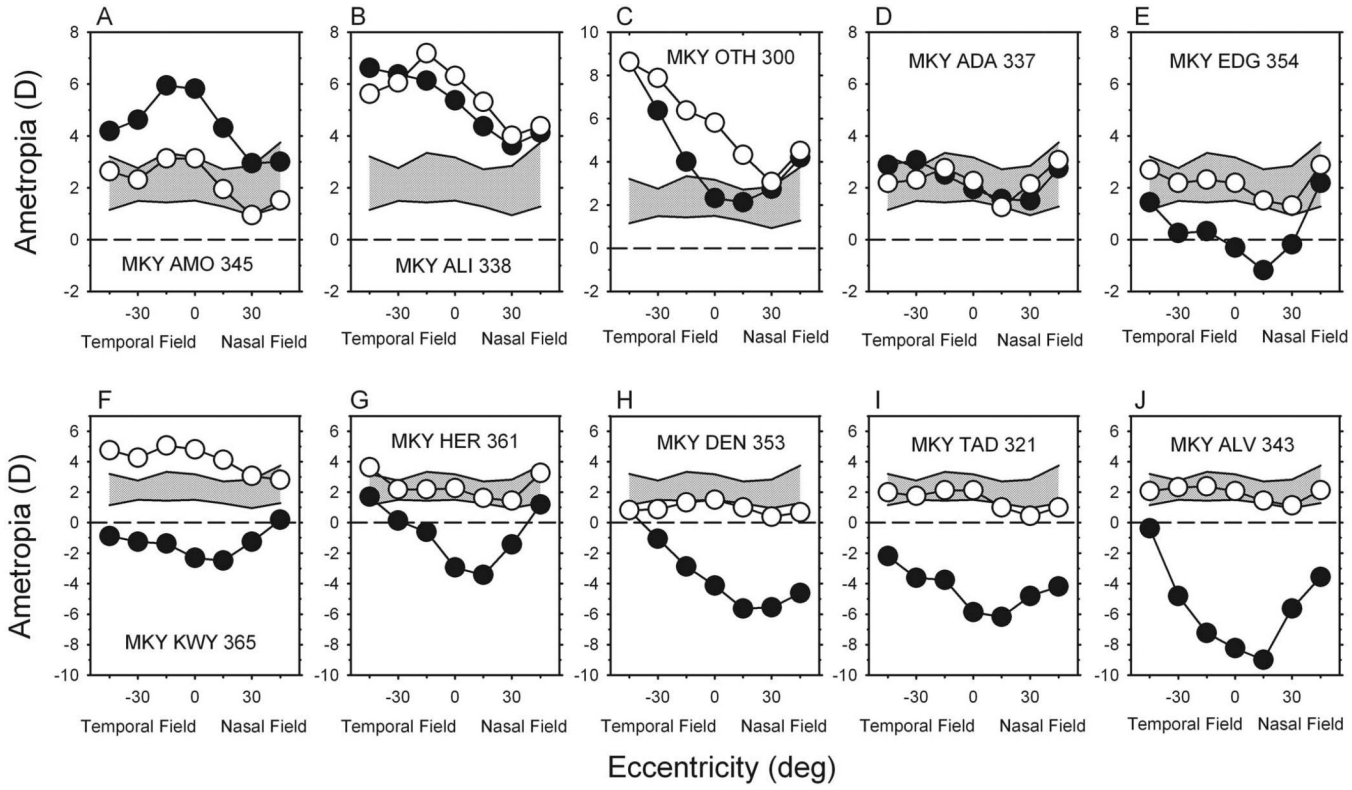

Figure 3.

(**A**–**J**) Animals are ordered according to the central ametropia of the treated eye. Spherical-equivalent refractive corrections obtained at the end of the treatment period plotted as a function of visual field eccentricity along the horizontal meridian for individual diffuser-reared monkeys. *Filled symbols*: treated eyes; *open symbols*: fellow eyes. *Diagonally cross-hatched areas* represent ±2 SD from the mean spherical-equivalent refractive corrections for the right eyes of the six control monkeys.

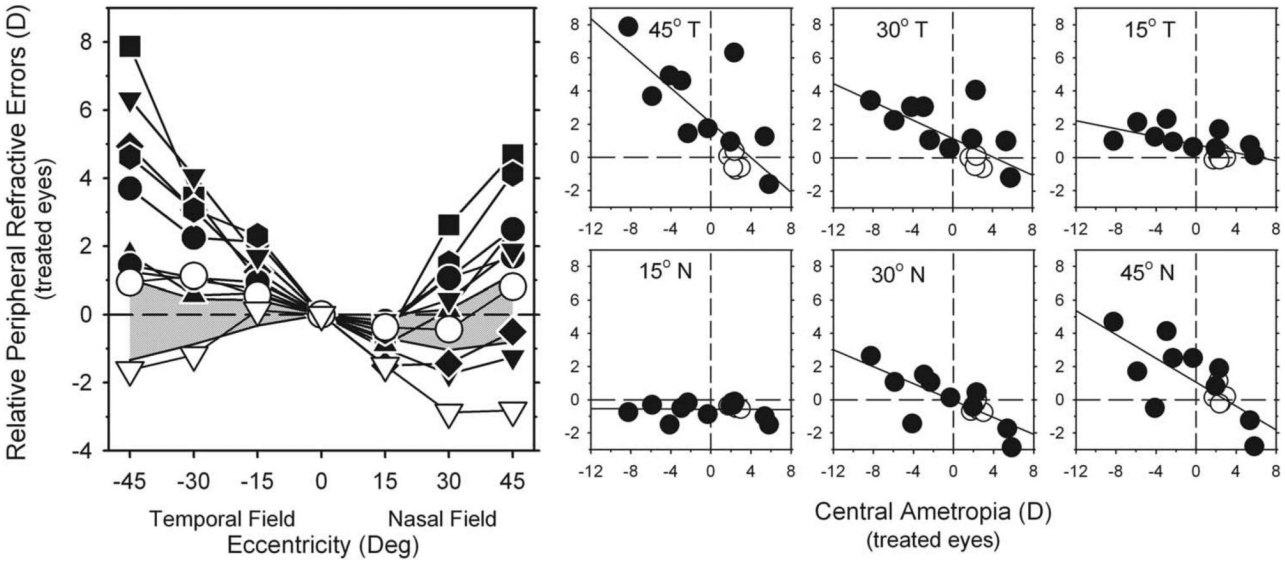

Figure 4.

Left: relative spherical-equivalent refractive corrections (peripheral – central ametropia) of the treated eyes plotted as a function of eccentricity along the horizontal meridian for individual diffuser-reared monkeys at the end of the treatment period. *Open triangles*: monkey that exhibited central hyperopic anisometropia. *Diagonally crosshatched area* represents ±2 SD from the mean relative refractive corrections for the control monkeys. *Right*: relative peripheral refractive corrections of the treated eyes plotted as a function of the central ametropia for each peripheral field eccentricity for the diffuser-reared (*filled symbols*) and control monkeys (*open symbols*). *Solid lines*: best-fitting regression lines.

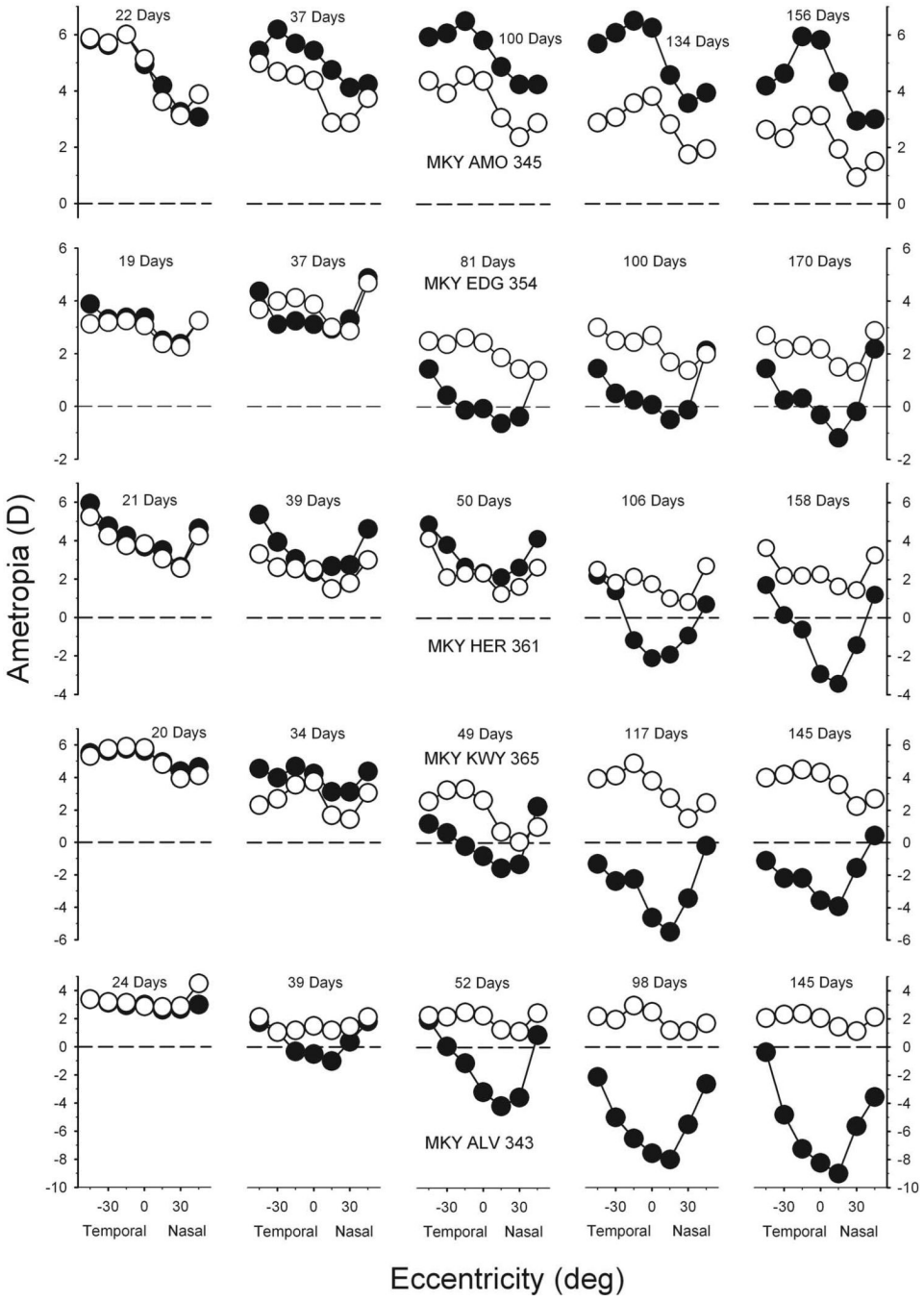

Figure 5.

Spherical-equivalent refractive corrections obtained at different times during the treatment period for five representative diffuser-reared monkeys plotted as a function of visual field eccentricity. Plots on the *left* were obtained at the onset of the treatment period; ages for the subsequent measures are shown in each plot. *Filled symbols*: treated eyes; *open symbols*: fellow eyes.

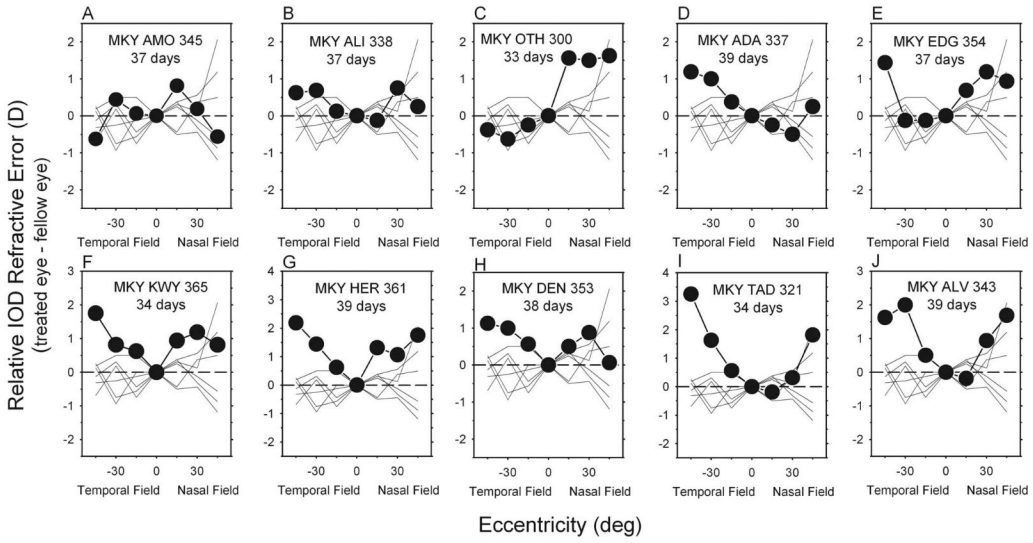

Figure 6.

(**A**–**J**) Normalized relative interocular differences in refractive corrections (treated eye – fellow eye) plotted as a function of eccentricity along the horizontal meridian for individual diffuser-reared monkeys (*filled symbols*). Data were obtained at the first measurement session after the onset of diffuser wear. *Thin lines*: relative interocular differences in spherical-equivalent refractive corrections (right eye – left eye) for control monkeys obtained at corresponding ages.

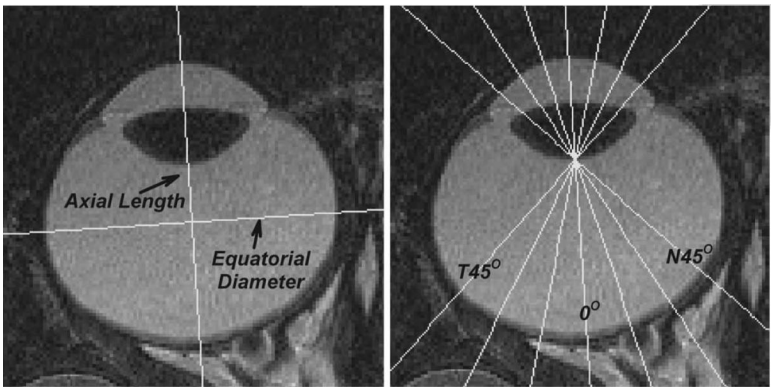

Figure 7.

MR images obtained in the horizontal plane at an age (143 days of age) corresponding to the end of the diffuser-rearing period for the right eye of a control monkey. *Left*: axial length was defined as the distance from the anterior corneal surface to the retina along the presumed optical axis. Equatorial diameter was defined as the greatest distance between the nasal and temporal retinas measured along a line that was perpendicular to the presumed optical axis. *Right*: vitreous chamber depths were measured from the posterior lens surface to the retina as a function of eccentricity from 45° nasally to 45° temporally in 15° intervals along the horizontal meridian.

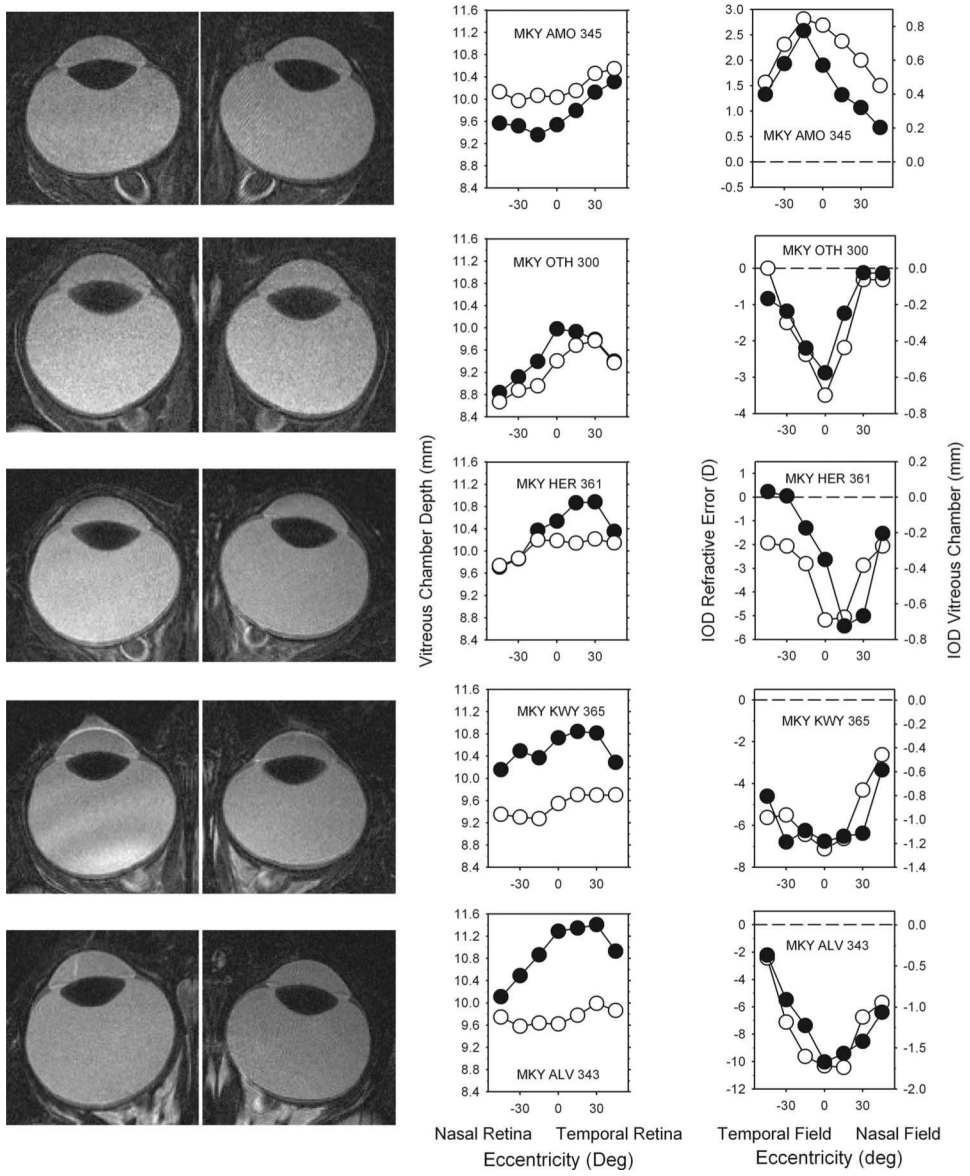

Figure 8.

Left: MR images obtained in the horizontal plane at the end of the diffuser-rearing period for the treated (*left*) and fellow eyes (*right*) of five representative form-deprived monkeys. *Middle*: vitreous chamber depths determined from the MR images are plotted as a function of retinal eccentricity for the treated eyes (*filled symbols*) and fellow eyes (*open symbols*). *Right*: comparisons of the interocular differences in refractive corrections (*open symbols* and *left ordinate scale*, treated eye – fellow eye) and vitreous chamber depth (*filled symbols* and *right ordinate scale*, fellow eye – treated eye) as a function of horizontal eccentricity.

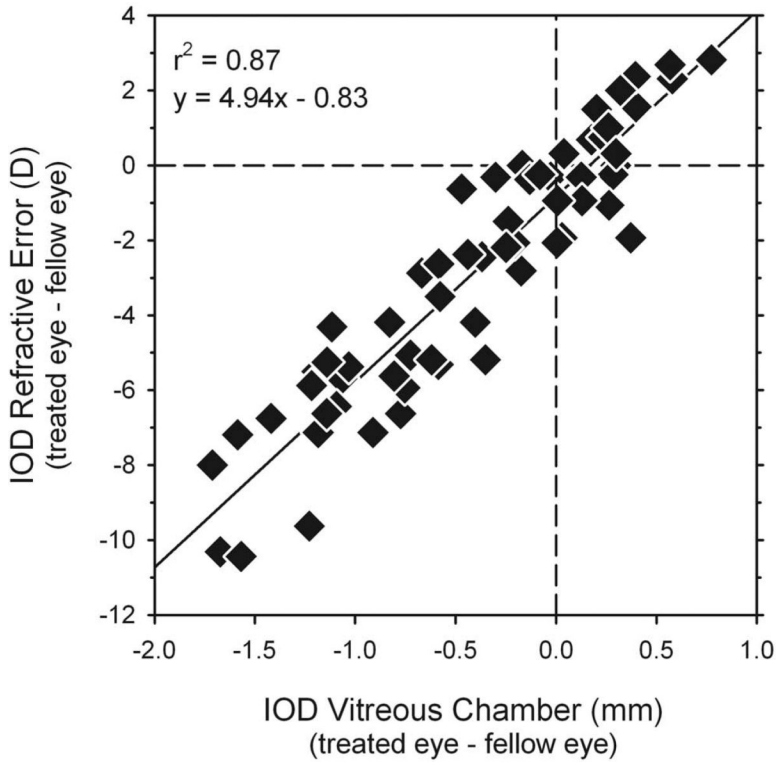

Figure 9.

Interocular differences in refractive error (treated eye – fellow eye) plotted as a function of the interocular differences in vitreous chamber depth (fellow eye – treated eye) determined from the MR images. Data are shown for all diffuser-reared monkeys and for all eccentricities along the horizontal meridian. The *solid line* represents best-fitting regression line.

Table 1

Axial Lengths and Equatorial Diameters

Animals	Refractive Error (D)			Axial Length (mm)			Equatorial Diameter (mm)		
	Treated Eye	Fellow Eye	IOD	Treated Eye	Fellow Eye	IOD	Treated Eye	Fellow Eye	IOD
Treated									
MKY AMO 345	+5.81	+3.13	2.69	15.80	16.38	–0.58	17.77	18.06	–0.29
MKY ADA 337	+1.94	+2.25	–0.31	16.56	17.00	–0.44	17.07	17.06	0.02
MKY ALI 338	+5.38	+6.31	–0.94	15.29	15.39	–0.10	16.25	16.52	–0.26
MKY OTH 300	+2.31	+5.81	–3.50	16.18	15.61	0.57	15.75	15.49	0.26
MKY HER 361	–2.94	+2.25	–5.19	16.80	16.58	0.23	17.16	17.37	–0.22
MKY DEN 353	–4.13	+1.50	–5.63	17.85	16.89	0.96	18.43	17.86	0.56
MKY KWY365	–2.31	+4.81	–7.13	16.56	15.82	0.73	16.93	16.48	0.45
MKY TAD 321	–5.88	+2.13	–8.00	18.39	16.70	1.69	18.24	17.26	0.98
MKY ALV 343	–8.25	+2.06	–10.31	17.82	16.02	1.79	17.41	16.80	0.61
Control	RE	LE	IOD	RE	LE	IOD	RE	LE	IOD
MKY 342	+2.12	+1.81	0.31	16.01	15.84	0.17	16.98	17.09	–0.11
MKY 344	+1.75	+1.87	–0.12	16.03	15.98	0.04	17.00	17.09	–0.09

Axial lengths and equatorial diameters were measured in the horizontal plane of the magnetic resonance images for both eyes of two control monkeys and nine form-deprived monkeys at ages corresponding to the treatment period. Spherical-equivalent refractive corrections for both eyes are also included in the table.